Matrix metalloproteinase-7 in urinary extracellular vesicles identifies rapid disease progression in autosomal dominant polycystic kidney disease

Heugten, M.H. van; Blijdorp, C.J.; Arjune, S.; Willigenburg, H. van; Bezstarosti, K.; Demmers, J.A.A.; ... ; DIPAK Consortium

Matrix Metalloproteinase-7 in Urinary Extracellular Vesicles Identifies Rapid Disease Progression in Autosomal Dominant Polycystic Kidney Disease

Martijn H. van Heugten,[1] Charles J. Blijdorp,[1] Sita Arjune,[2,3,4] Hester van Willigenburg,[1] Karel Bezstarosti,[5] Jeroen A. A. Demmers,[5] Usha Musterd-Bhaggoe,[1] Esther Meijer,[6] Ron T. Gansevoort,[6] Robert Zietse,[1] Sikander Hayat,[7] Rafael Kramann,[1,7,8] Roman-Ulrich Müller,[2,3,4] Mahdi Salih,[1] and Ewout J. Hoorn,[1] On behalf of the DIPAK Consortium*

Due to the number of contributing authors, the affiliations are listed at the end of this article.

ABSTRACT

Background In ADPKD, there is an unmet need for early markers of rapid disease progression to facilitate counseling and selection for kidney-protective therapy. Our aim was to identify markers for rapid disease progression in uEVs.

Methods Six paired case–control groups (n=10–59/group) of cases with rapid disease progression and controls with stable disease were formed from two independent ADPKD cohorts, with matching by age, sex, total kidney volume, and genetic variant. Candidate uEV biomarkers were identified by mass spectrometry and further analyzed using immunoblotting and an ELISA. Single-nucleus RNA sequencing of healthy and ADPKD tissue was used to identify the cellular origin of the uEV biomarker.

Results In the discovery proteomics experiments, the protein abundance of MMP-7 was significantly higher in uEVs of patients with rapid disease progression compared with stable disease. In the validation groups, a significant >2-fold increase in uEV-MMP-7 in patients with rapid disease progression was confirmed using immunoblotting. By contrast, no significant difference in MMP-7 was found in whole urine using ELISA. Compared with healthy kidney tissue, ADPKD tissue had significantly higher MMP-7 expression in proximal tubule and thick ascending limb cells with a profibrotic phenotype.

Conclusions Among patients with ADPKD, rapid disease progressors have higher uEV-associated MMP-7. Our findings also suggest that MMP-7 is a biologically plausible biomarker for more rapid disease progression.

JASN 35: 321–334, 2023. doi: https://doi.org/10.1681/ASN.0000000000000277

Received: May 17, 2023 **Accepted:** November 12, 2023.
Published Online Ahead of Print: December 11, 2023.

*The DIPAK consortium includes: Charles Blijdorp, Esther Meijer, Ronald Gansevoort, Robert Zietse, Mahdi Salih, Ewout Hoorn, D.J.M. Peters, and M. Losekoot (Leiden University Medical Center), J.W. de Fijter (Antwerp University Hospital), F.W. Vissers (Zorggroep Twente, Almelo), J.P.H. Drenth, T. Nijenhuis, and J. Wetzels (Radboud University Medical Center, Nijmegen), M.D.A. van Gastel (University Medical Center Groningen).

M.H.v.H., C.J.B., M.S., and E.J.H. contributed equally to this work.

Correspondence: Prof. Ewout J. Hoorn, Department of Internal Medicine, Division of Nephrology and Transplantation, Erasmus Medical Center, PO Box 2040, 3000 CA Rotterdam, The Netherlands. Email: e.j.hoorn@erasmusmc.nl

INTRODUCTION

Autosomal dominant polycystic kidney disease (ADPKD) is the most common inherited kidney disease and is primarily caused by pathogenic variants of the *PKD1* or *PKD2* gene.[1,2] The disease is characterized by the development of multiple bilateral kidney cysts frequently leading to kidney failure. The rate of disease progression in ADPKD is highly variable, even within families that share the same genetic variant, but tends to be most severe in those with a *PKD1* variant.[3] Several prognostic classifications have been developed to predict disease progression, of which the Mayo classification and the Predicting Renal Outcomes in ADPKD (PRO-PKD) score are most commonly used.[4–6] These prognostic models rely on height-adjusted total kidney volume (htTKV) or *PKD* gene analysis. Actual disease progression still varies considerably within predicted categories, limiting the value of these models at an individual patient level.[4,6] Therefore, there is an unmet need for novel biomarkers that can identify patients with rapid disease progression. The advent of tolvaptan as a treatment option for patients with ADPKD further highlights this need. A well-performing prognostic biomarker could avoid unnecessary treatment and potential side effects in patients with a favorable kidney prognosis.

Urinary extracellular vesicles (uEVs) represent an attractive source of kidney biomarkers that contain proteins and RNAs from their parent cells. uEVs are nanoparticles that bud and release from plasma cell membranes (microvesicles and apoptotic bodies) or are released from multivesicular bodies (exosomes). uEV analysis allows for the noninvasive assessment of both physiological and pathophysiological processes in the epithelial cells lining the nephron and urinary tract.[7,8] The isolation and characterization of uEVs has, therefore, become a powerful approach to identify biomarkers for kidney diseases, including ADPKD.[8,9] Several groups, including ours, have previously performed proteomic studies of uEVs to identify proteins unique to ADPKD and its severity.[9–15] These studies, however, did not yet address whether uEVs can be used to differentiate patients with ADPKD on the basis of their rate of disease progression. Here, we present the results of a shotgun proteomics study aimed at identifying uEV proteins that distinguish patients with ADPKD who subsequently developed rapid disease progression from those who had stable disease. Our findings suggest that uEV-associated matrix metalloproteinase 7 (MMP-7) discriminates rapid disease progression from stable disease in patients with ADPKD.

Significance Statement

There is an unmet need for biomarkers of disease progression in autosomal dominant polycystic kidney disease (ADPKD). This study investigated urinary extracellular vesicles (uEVs) as a source of such biomarkers. Proteomic analysis of uEVs identified matrix metalloproteinase 7 (MMP-7) as a biomarker predictive of rapid disease progression. In validation studies, MMP-7 was predictive in uEVs but not in whole urine, possibly because uEVs are primarily secreted by tubular epithelial cells. Indeed, single-nucleus RNA sequencing showed that MMP-7 was especially increased in proximal tubule and thick ascending limb cells, which were further characterized by a profibrotic phenotype. Together, these data suggest that MMP-7 is a biologically plausible and promising uEV biomarker for rapid disease progression in ADPKD.

METHODS

Setting and Patients

Patients with rapid disease progression and stable disease were selected from two independent cohorts, including the Developing Intervention Strategies to Halt Progression of Autosomal Dominant Polycystic Kidney Disease (DIPAK) cohort from the Netherlands and the Cologne cohort from Germany (Figure 1). The discovery proteomics experiments and internal validation experiments were performed in patients selected from the DIPAK cohort while the external validation experiments were performed in patients selected from the Cologne cohort. Six case–control groups were formed, including patients with rapid disease progression (eGFR decline $\geq$4 ml/min per 1.73 m^2 per year) and patients with stable disease (eGFR decline $\leq$2 ml/min per 1.73 m^2 per year). All cases and controls were matched 1:1 by age, sex, baseline eGFR, htTKV, and genetic variant. From the DIPAK cohort two case–control groups (groups 1 and 2) were formed for the discovery proteomics experiments, and two additional groups were formed for the internal validation experiments using immunoblotting and whole-urine ELISA (groups 3 and 4). The reason to use two groups for discovery was that we used a tandem mass tag (TMT) labeling approach that at the time restricted group size to ten patients. From the Cologne cohort, two case–control groups (groups 5 and 6) were formed for external validation, including one with baseline eGFR 30–60 ml/min per 1.73 m^2 (group 5) and one with baseline eGFR 60–90 ml/min per 1.73 m^2 (group 6). The DIPAK cohort was established from an open-label randomized clinical trial designed to examine the effect of lanreotide on disease progression in patients with ADPKD with an eGFR of 30–60 ml/min per 1.73 m^2.[16] Baseline and follow-up measurements of this study, including BP, body weight, magnetic resonance imaging-based htTKV, and kidney function, have been described previously.[17] The Cologne cohort enrolls patients with ADPKD not requiring kidney replacement therapy (trial registration numbers NCT02497521 and DRKS00008910). Both the DIPAK and Cologne cohorts were approved by the institutional review boards, and informed consent was obtained from all participants.

Sample Collection and uEV Isolation

Fifty milliliter spot urine samples that had been stored at −80°C after addition of a protease inhibitor were used for uEV isolation. uEVs were isolated using a differential ultracentrifugation protocols that were essentially the same

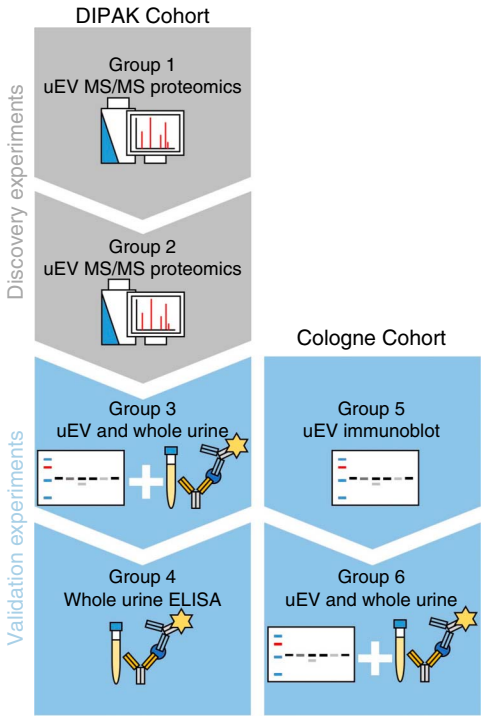

Figure 1. Study design showing the two ADPKD cohorts from DIPAK and Cologne and the six case–control groups that were formed for the individual studies. In the discovery experiments (gray shading), uEVs were analyzed using MS/MS quantitative proteomics with TMT labeling (groups 1 and 2). In the validation experiments (blue shading) immunoblotting and/or an ELISA on whole urine were used (groups 3–6). ADPKD, autosomal dominant polycystic kidney disease; TMT, tandem mass tag; uEV, urinary extracellular vesicle.

for the two cohorts with minor differences.[18–20] In brief, both protocols used low-speed centrifugation steps before and after freezing. The ultracentrifugation steps to pellet the uEVs were 120 minutes at 200,000×*g* (group 1), 160 minutes at 150,000×*g* (groups 2 and 3, because of a restriction of the maximum revolutions per minute of the rotor), and 60 minutes at 200,000×*g* (groups 5 and 6). Dithiothreitol (200 mg/ml) was used to dissociate uromodulin polymers in the DIPAK cohort but not in the Cologne cohort. The final supernatant was discarded, and the uEV pellet was dissolved in 150 μl PBS (DIPAK cohort) or 40 μl 8 M urea buffer (Cologne cohort) and stored at −80°C until analysis.

Mass Spectrometry

uEV isolates from our first two groups were lyzed in 100 mM triethylammonium bicarbonate buffer containing 1% sodium deoxycholate, 1% SDS, and 2% Triton X100 by sonication for 10 minutes using a bioruptor (Diagenode). Proteins were quantified using the bicinchoninic acid assay protein kit (ThermoFisher Scientific/Pierce, catalog 23225). Twenty microgram of protein was digested using the SP3 protocol,[21] and individual peptide samples were isobarically labeled using the TMT 10-plex isobaric reagent kit (ThermoFisher Scientific, A34808) according to the supplier's instructions. TMT-labeled samples were then combined for each group and analyzed using nanoflow liquid chromatography tandem mass spectrometry on an EASY-nLC coupled to an Orbitrap Lumos Tribid mass spectrometer (ThermoFisher Scientific) operating in positive mode. Peptides were separated on a ReproSil-C18 reversed phase column (Dr. Maisch; 25 cm×75 μm) using a linear gradient of 0%–80% acetonitrile (in 0.1% formic acid) during 90 minutes at a flow rate of 250 nl/min. Spectra were acquired according to a data-dependent acquisition regimen in continuum mode; fragmentation of the peptides was performed by higher-energy collision dissociation using the multinotch synchronous precursor selection MS3 reporter ion-based quantification method. Peptide spectra were analyzed using Proteome Discoverer 2.5 (ThermoFisher, Scientific), and total peptide abundances were normalized for all TMT channels before protein abundance computation and further statistical processing in R. Groups 1 and 2 were both quantified in their own pooled TMT analysis, maximizing sample comparability within experiments. Identified proteins were compared with the Vesiclepedia uEV proteome database.[22]

Immunoblotting

To validate the mass spectrometry findings, we performed immunoblots using primary antibodies against MMP-7 (1:100, Santa Cruz, SC-515703; 1:200, Santa Cruz, SC-80205), charged multivesicular body protein 4a (CHMP4A) (1:100, Santa Cruz, SC-514869), and secondary horseradish peroxidase-conjugated goat anti-mouse IgG antibodies (1:3000, Biorad, L005680). uEV isolates from groups 3, 5, and 6 were mixed with Laemmli buffer for immunoblot analysis, and samples were loaded relative to urine creatinine.[23] We used Criterion tris-glycine extended precast polyacrylamide midi gels (Biorad), and proteins were transferred to membranes using a Trans-Blot Turbo (Biorad). Membranes were blocked using 5% bovine serum albumin in tris-buffered saline with 0.1% Tween 20 (Sigma-Aldrich) for 1 hour and visualized using an Amersham AI600 Chemiluminescent imager (GE Healthcare) and Clarity Western enhanced chemiluminescence substrate (Biorad). Acquisition images were processed using Image Studio version 5.2 (LI-COR Biotechnology), and background normalized values were exported to R for statistical analysis. Densitometry values of MMP-7 and CHMP4A from group 3 were also extrapolated to 24-hour protein excretion by correcting for the individual's 24-hour creatinine excretion.[23]

Whole-Urine ELISA

To compare the performance of uEV-specific MMP-7 to unprocessed urine, we measured whole-urine MMP-7 in groups 3, 4, and 6 using the commercial Human Total MMP-7 DuoSet ELISA (DY907, R&D Systems) according to the vendor's instructions. In brief, plates were coated using 100 μl of 180 μg/ml capture antibody and incubated overnight at room

temperature. Plates were then washed and blocked, and samples were thawed at room temperature, vortexed, and diluted ten times in reagent buffer before 100 μl of diluted sample was loaded per well in duplicate and incubated for 2 hours at room temperature. After sample removal and washing, 100 μl of detection antibody solution was added and incubated at room temperature for 2 hours. The detection antibody solution was removed and plates were washed before 100 μl of working dilution streptavidin-HRP was added and incubated at room temperature for 20 minutes in the dark. Plates were again aspirated and washed before 100 μl of substrate solution was added, incubated for 20 minutes at room temperature in the dark, and finally 50 μl of stop solution was added, and optical density measured at 450 nm with the absorption at 540 nm subtracted.

Small Nuclear Ribonucleic Acid Sequencing

Small nuclear ribonucleic acid sequencing data from one of our recent studies[24] were analyzed for MMP-7. In this previous study, healthy kidney tissue from kidney donor biopsies (n=2) and ADPKD kidney tissue acquired after nephrectomy in preparation for kidney transplantation (n=3) was homogenized using nuclei isolation buffer (EZ lysis buffer, NUC101, Sigma-Aldrich) to form single-cell suspension as previously described.[24–26] Free nuclei suspensions were enriched using a SH800 cell sorter (Sony Biotechnology) before nuclei in suspension were loaded into the chromium controller (10×, Genomics, PN-120223′) on a Single Cell B chip (10× Genomics, PN-120262) and processed following the manufacturer's instructions to produce single-cell gel beads. The sequencing library was generated using the Chromium Single cell 3′ reagent Kit v3 (10× Genomics, PN-120262) and Chromium i7 Multiplex Kit (10× Genomics, PN-1000092). Libraries were sequenced on NovaSeq targeting 50,000 reads per cell as described previously.[25,26] Cells were annotated using previously reported marker genes of the kidney precision medicine project.[27] For each cell type, we calculated the percentage of MMP-7–expressing cells and the average expression for each cell type. Finally, we compared MMP-7–positive and MMP-7–negative cells for gene expression of selected profibrotic genes (using a cutoff of 0 transcripts).[28]

Statistical Analysis

Patient baseline characteristics other than variables used for matching were compared using the Student t tests and chi-square tests, as appropriate. For all groups, the eGFR slope was calculated using univariable linear regression. Tandem mass spectrometry-identified and TMT-normalized proteins were only used for statistical analysis when they were reliably quantified for all cases. Protein abundances were normalized using the Bioconductor *vsn*-package for R to address the observed dependence of variance on protein abundance means.[29,30] Protein abundances were compared between groups using two-tailed independent samples Student t tests, and protein fold changes were calculated dividing the mean difference in abundance by the mean of the stable disease as the reference group. Pathway analysis was performed in group 1 using the *ReactomePA* package for R using the Reactome pathway database (version 1.34.0) and the Vesiclepedia uEV proteome as background.[31,32] Immunoblot optical densities of MMP-7 and CHMP4A of group 3 were compared using an independent samples t test, with values for groups 5 and 6 compared using the Wilcoxon rank sum test because of the non-normal distribution of the data. The ELISA MMP-7 abundance of groups 3, 4, and 6 was divided by urinary creatinine concentration and compared between rapid progressive and stable cases using an independent samples t test. The ELISA MMP-7 abundance of group 4 was further explored using linear regression, correlating the individual eGFR slope to the creatinine-corrected urinary MMP-7 abundance. In addition to the univariable model, a multivariable analysis adding a plate-specific factor, patient sex, age, baseline eGFR, and truncating or nontruncating *PKD1* variant was performed. To compare the associations of uEV MMP-7 and whole-urine MMP-7 with eGFR loss over time, the uEV immunoblot and whole-urine ELISA measurements in groups 3 and 6 were used to calculate receiver operating characteristic curves and compared using the pROC package in R.[33]

Table 1. Selected baseline characteristics

Characteristic	Group 1 n=10	Group 2 n=10	Group 3 n=24	Group 4 n=59	Group 5 n=24	Group 6 n=24
Cohort	DIPAK	DIPAK	DIPAK	DIPAK	Cologne	Cologne
Baseline eGFR range, ml/min per 1.73 m^2	30–60	30–60	30–60	30–60	30–60	60–90
Age, yr	50.1 (7.0)	43.3 (5.1)	48.6 (8.7)	48.7 (5.7)	51.0 (10.4)	44.4 (9.0)
Female sex, %	60	40	58	76	50	50
PKD1 variant, %	100	100	80	100	46	46
Truncating *PKD1* variant, %	100	100	30	59	42	33
PRO-PKD score	4.8 (2.1)	6.2 (1.8)	3.8 (2.4)	4.4 (1.6)	3.9 (2.7)	3.8 (3.3)
Mayo classification score	3.1 (0.7)	3.6 (1.0)	3.2 (0.8)	3.1 (0.7)	3.5 (1.1)	3.4 (1.2)
htTKV baseline, mL/m	857 (282)	1398 (875)	1069 (670)	916 (4.64)	1790 (1301)	1049 (580)

htTKV, height-adjusted total kidney volume.

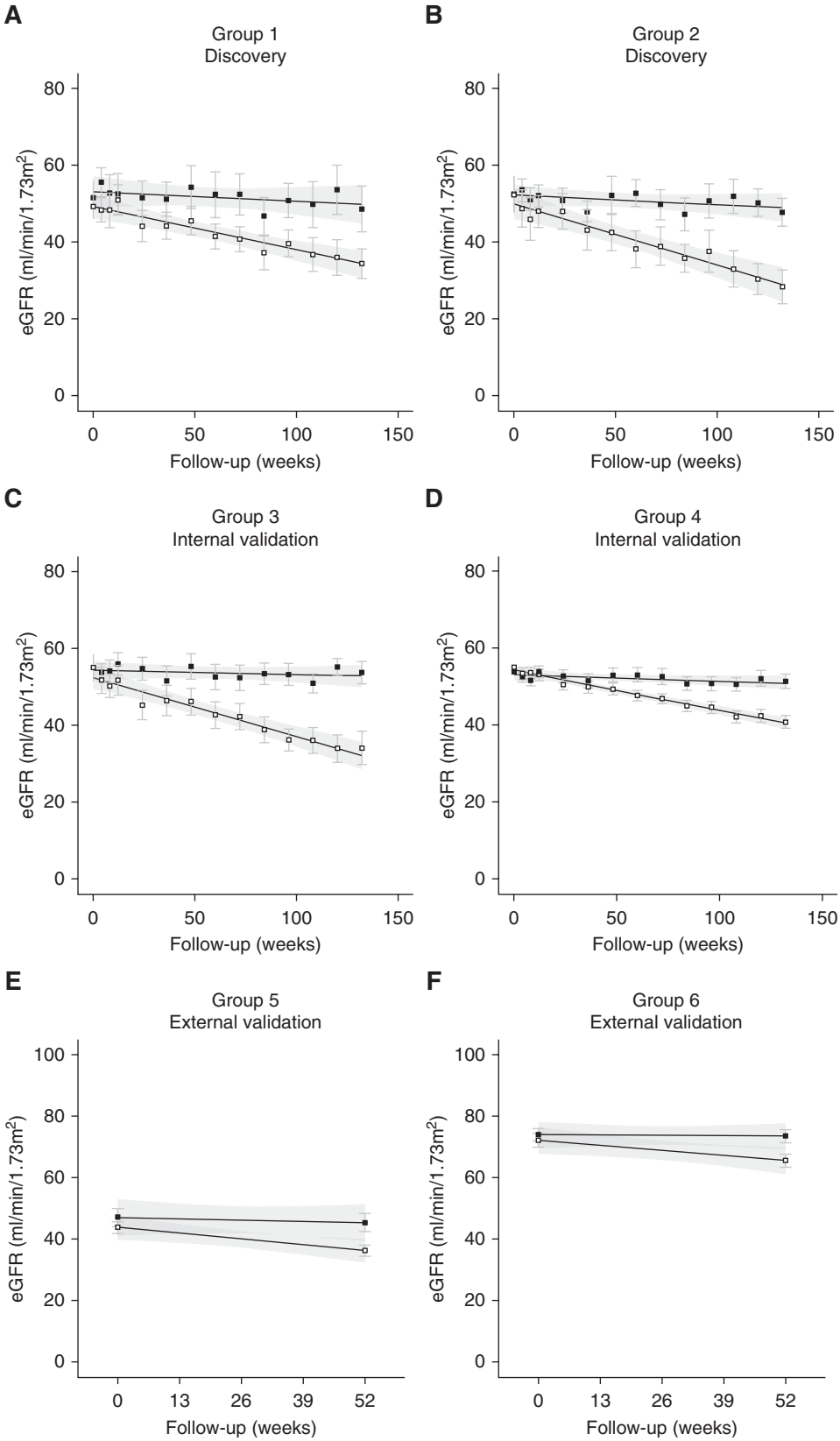

Figure 2. eGFR over time in the six groups. eGFR is depicted as mean±SEM with fitted linear regression including the 95% confidence interval in gray. eGFR over 2.5 years of follow-up is shown for the discovery Groups 1 and 2 (panels A and B), internal validation Groups 3 and 4 (panels C and D) and the external validation Groups 5 and 6 (panels E and F).

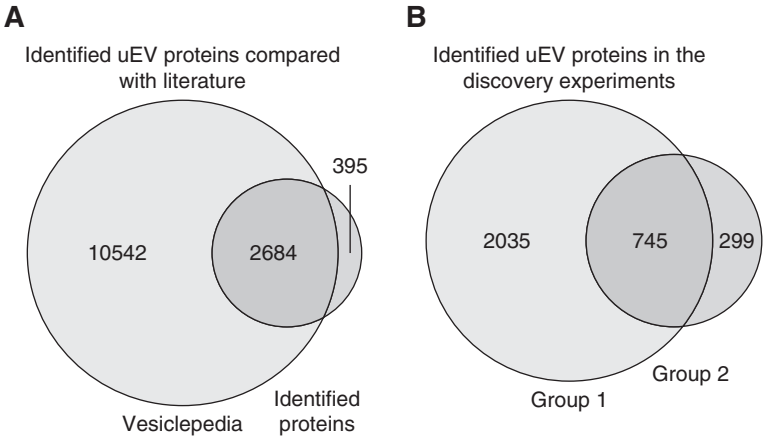

Figure 3. Total number of proteins identified in the MS/MS experiments. (A) Venn diagram comparing the proteins identified in isolated uEVs within the MS/MS experiments combined with the extracellular proteome reported on Vesiclepedia. (B) Venn diagram comparing the proteins identified in isolated uEVs in the MS/MS experiments (rapid disease progression versus stable disease in discovery groups 1 and 2).

RESULTS

Clinical Characteristics

The clinical characteristics of the six case–control groups are shown in Table 1 and Supplemental Tables 1–4, and the eGFR decline over time is shown in Figure 2. The four DIPAK case–control groups included patients who primarily carried the *PKD1* variant and who had an age between 42 and 51 years and eGFR between 49 and 55 ml/min per 1.73 m^2. The two case–control groups from the Cologne cohort were largely similar, except for a lower percentage of patients with the *PKD1* variant and one group with higher eGFR (between 60 and 90 ml/min per 1.73 m^2). Other characteristics, including Mayo classification score and the use of renin-angiotensin inhibitors, were largely similar between groups (Supplemental Tables 1–4).

Protein Identification and Pathway Analysis

uEV proteomic analysis of groups 1 and 2 identified 2780 and 1044 unique proteins. Of the 3079 unique uEV proteins identified in both groups, the majority (87%) has been reported previously in the Vesiclepedia proteome database (Figure 3A). The overlap of identified uEV proteins in groups 1 and 2 is shown in Figure 3B. To determine if uEV proteins with different abundances in patients with rapid disease progression compared with stable disease reflect altered biological processes, we performed pathway analysis in group 1. In the Reactome database, we identified 176 enriched pathways, including nested pathways (Supplemental Data). These pathways not only include protein folding and extracellular signal-regulated kinase / mitogen-activated protein kinase functions but also several signaling pathways, including Wnt-signaling, insulin and glucagon signaling, fibroblast growth factor receptor 2 and fibroblast growth factor receptor 4, and prostacyclin and thromboxane signaling. All of these pathways have previously been implicated in the pathophysiology of ADPKD.[24,34–37] All MS data are available on ProteomeXchange through the PRIDE database (identifier PXD042533).

Differential Expression of MMP-7 in Rapid Disease Progression

In group 1, we identified 65 uEV proteins, and in group 2, we identified 36 uEV proteins with significantly different abundances between patients with rapid disease progression and stable disease (Figure 4, A and B, Figure 1, and Supplemental Tables 5 and 6). MMP-7 and CHMP4A were consistently higher and lower in groups 1 and 2, respectively (Figure 4, C–F and Supplemental Data). Internal validation of the tandem mass spectrometry results by immunoblotting using uEVs from group 3 confirmed a significantly higher abundance of MMP-7 in patients with rapid disease progression compared with patients with stable disease (Figure 5, A and B). In contrast to the mass spectrometry data, however, CHMP4A when analyzed with immunoblotting was *higher* in patients with rapid disease progression than in patients with stable disease (Figure 5, A and C). We hypothesized that the normalization strategy by total protein for mass spectrometry and by urine creatinine for immunoblot could explain the opposite direction of change in CHMP4A. Indeed, when the immunoblots were loaded with normalization for the uEV marker CD9, the higher abundance of MMP-7 in patients with rapid disease progression persisted (Supplemental Figure 2), whereas no difference in CHMP4A was found (data not shown). We, therefore, concluded that MMP-7 was the most robust and reproducible uEV-biomarker, which was then further analyzed. We extrapolated the MMP-7 abundance to 24-hour excretion and found that it remained significantly higher in those with rapid disease

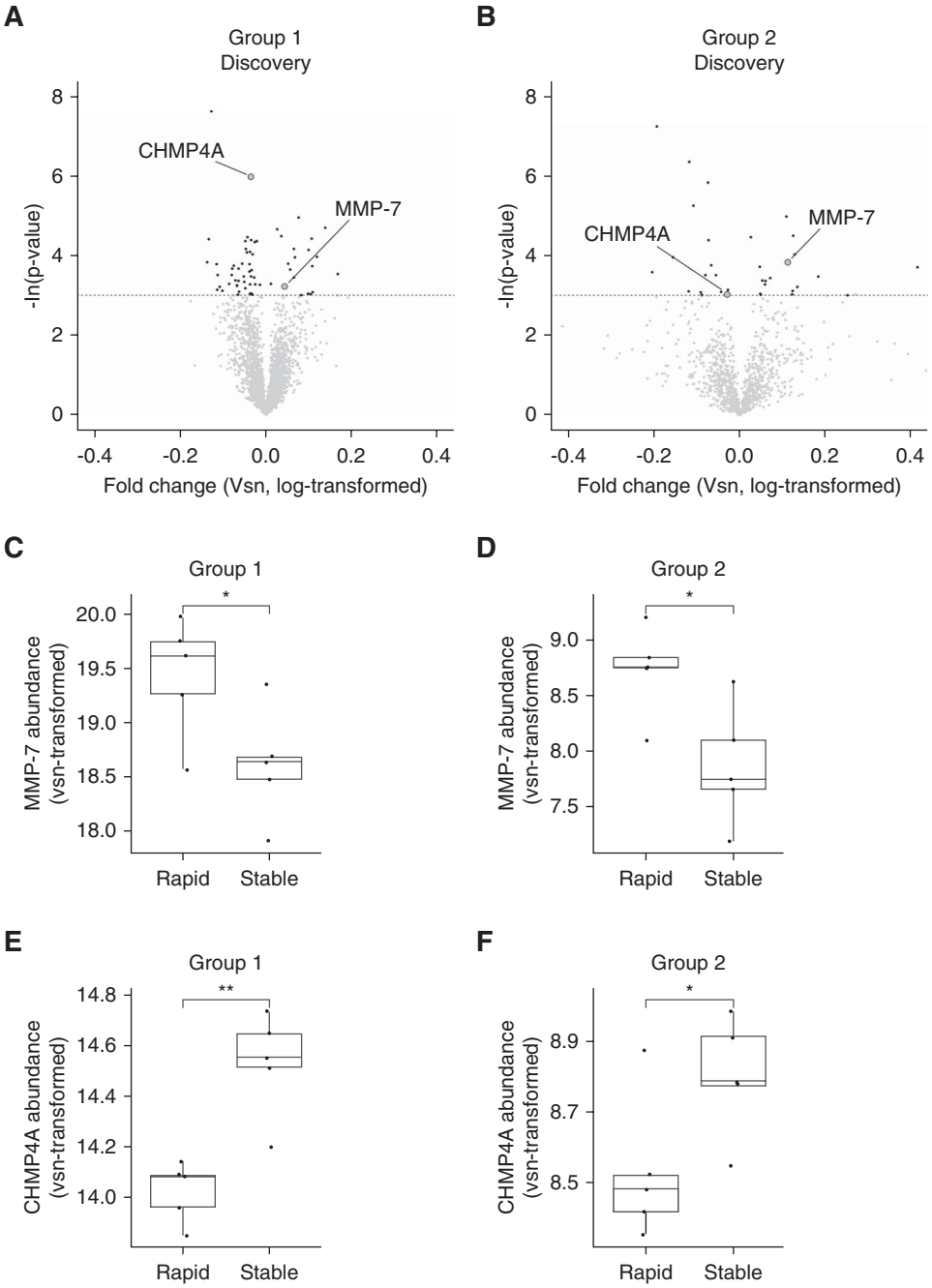

Figure 4. Identification of uEV-MMP-7. Volcano plots for the comparison of protein abundance in isolated uEVs of patients with rapid disease progression versus stable disease in (A) group 1 and (B) group 2. *X*-axis depicts *vsn*-normalized abundance ratio (rapidly progressive/stable), which includes a log transformation. *Y*-axis depicts naturally log-transformed *P* values of the Student *t* test, with cutoff at −Ln(0.05). Significantly different proteins ($P < 0.05$) are marked in darker gray. Abundance of biomarker candidates (C and D) MMP-7 and (E and F) CHMP4A in the MS/MS experiments of groups 1 and 2. Abundances were *vsn*-normalized, which includes log transformation. *$P < 0.05$, **$P < 0.01$ by the Student *t* test. CHMP4A, charged multivesicular body protein 4a; MMP-7, matrix metalloproteinase 7.

progression (Figure 5D). In the two external validation groups (groups 5 and 6), uEV-MMP-7 was also significantly higher in patients with rapid disease progression compared with stable disease (Figure 5, E and F). We did see more variability in groups 5 and 6 than in group 3. Lower than expected MMP-7 abundance in patients with rapid disease progression may be attributable to initiation of CKD progression at a later time than the baseline collection or the presence of MMP-7

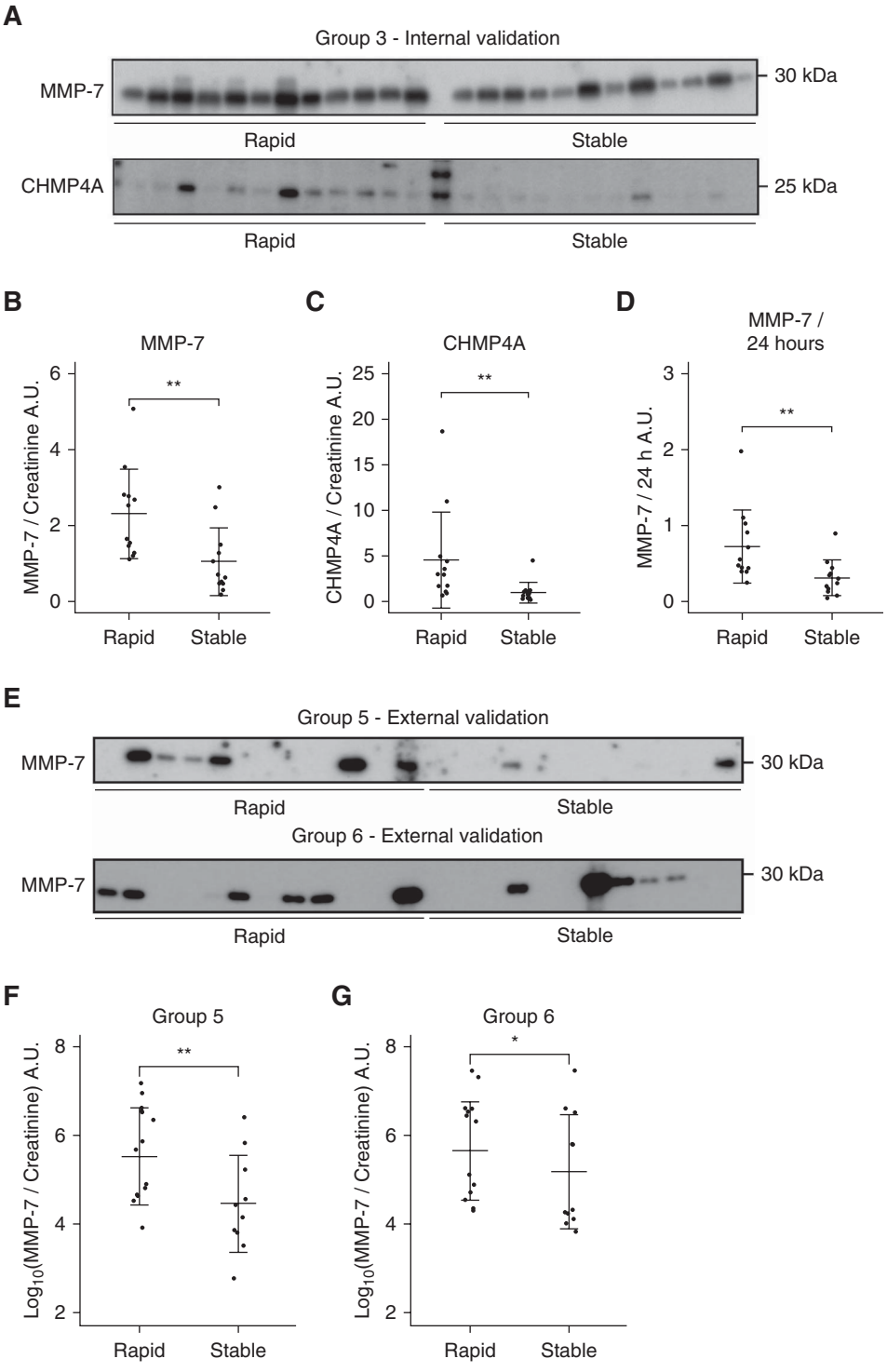

Figure 5. Immunoblot analysis of MMP-7 and CHMP4A in uEVs. (A) Immunoblot analysis of MMP-7 and CHMP4A in internal validation group 3 including (B and C) densitometry. (D) Daily urinary MMP-7 excretion was assessed by extrapolating uEV-MMP-7 abundance using each individual patient's 24-hour urinary creatinine excretion. (E–G) The findings were confirmed in the two external validation groups (groups 5 and 6). *$P < 0.05$, **$P < 0.01$ by the Student *t* test for groups 3 and 4 and the Wilcoxon rank sum test for groups 5 and 6 because of the non-normal distribution of MMP-7 abundance data.

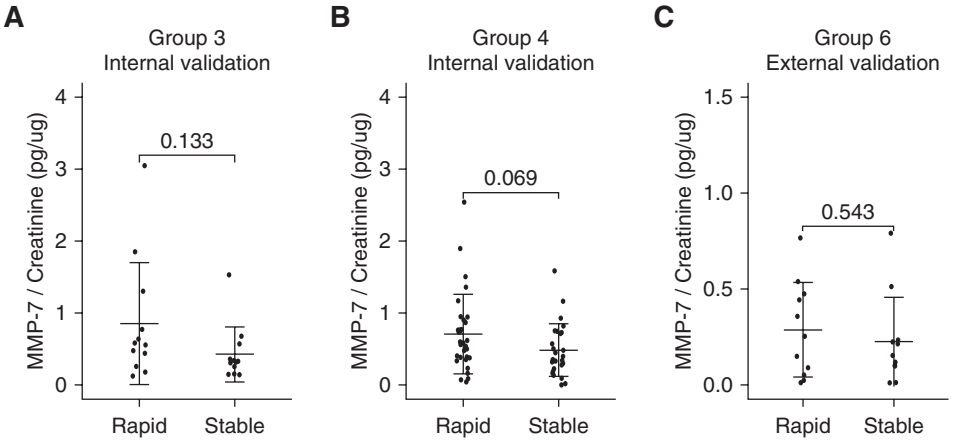

Figure 6. MMP-7 abundance in whole urine. ELISA of whole-urine MMP-7 shows a nonsignificantly higher creatinine-corrected MMP-7 in patients with rapid disease progression compared with patients with stable disease in (A and B) the two internal validation groups (groups 3 and 4) and (C) one of the external validation groups (group 6).

proteolytic fragments that were undetectable by immunoblot. Conversely, higher MMP-7 abundance in patients with stable disease may be attributable to an intercurrent episode of AKI.

MMP-7 Whole-Urine ELISA Does Not Distinguish Rapid from Slow Disease Progression

We determined the utility of a whole-urine ELISA for the high-throughput identification of patients with rapid disease progression or stable disease. In spot urine samples from case–control groups 3, 4, and 6, MMP-7 protein levels corrected for urine creatinine (MMP-7/creatinine) were higher in patients with rapid disease progression compared with patients with stable disease, but this difference did not reach statistical significance (Figure 6, A–C). In a linear regression analysis, MMP-7/creatinine did significantly correlate with the decline in eGFR in all models, but with a low R^2 value of 0.01 (Table S7). Next, we compared the performance of uEV and whole-urine MMP-7 and found that the area under the receiver operating characteristic curve of uEV-MMP-7 was significantly greater than for the whole-urine MMP-7 (group 3: 0.77 versus 0.69, $P = 0.05$; group 6: 0.83 versus 0.56, $P = 0.01$, Supplemental Figure 3). The correlation between uEV and whole-urine MMP-7 was weak and not statistically significant (Supplemental Figure 4).

Single-Nucleus RNA Sequencing

We analyzed snRNA sequencing of the human kidney in both healthy controls and patients with ADPKD to identify the cellular origin of uEV MMP-7 (Figure 7, A–C). We found a markedly higher MMP-7 abundance in ADPKD kidney tissue compared with healthy control tissue (Figure 7D). In the human kidney, MMP-7 appears to be primarily expressed in cells of the proximal tubule and thick ascending limb (TAL), as well as a smaller proportion of connecting duct and collecting duct cells (Figure 7, C and D). Comparing healthy control with ADPKD tissue showed that in ADPKD proximal tubular and TAL cells MMP-7 expression was 1.5 and 2.0 times higher, respectively (adjusted P value < 0.01 for both, Figure 7, B and C). This was due to both an increase in the proportion of MMP-7–expressing cells and the expression of MMP-7 per positive cell (Figure 7D). We also observed a higher expression of profibrotic genes in MMP-7+ proximal tubular and TAL cells, especially doublecortin domain containing 2 (DCDC2) and prominin-1 (PROM1) (Figure 8, A–C). To further analyze MMP-7 in health and in kidney disease, we reanalyzed the uEV proteomics data from one of our previous studies in which we compared uEV protein abundances of patients with ADPKD with healthy individuals and those with non-ADPKD CKD.[9] In this previous data set, MMP-7 was undetectable in healthy individuals, whereas it was detectable and 13-fold higher in ADPKD compared with non-ADPKD CKD (Supplemental Figure 5).

DISCUSSION

Here, we aimed to identify and validate novel uEV biomarkers that may help to identify rapid disease progression in patients with ADPKD. Using a step-wise approach with six matched case–control groups, we identified MMP-7 as a promising new uEV biomarker. MMP-7 performed better as a biomarker when analyzed in uEVs compared with whole urine, which may be due to the fact that uEVs are primarily secreted by tubular epithelial cells. Using snRNA-sequencing data, we show that MMP-7 is significantly higher expressed in ADPKD kidney tissue than in healthy kidney tissue, especially in proximal tubular and TAL cells with a profibrotic phenotype.

MMP-7 is an endopeptidase MMP with proteolytic activity against a wide range of extracellular proteins that regulate different biological processes such as apoptosis, fibrosis, and inflammation.[38–41] MMP-7 was previously identified at the

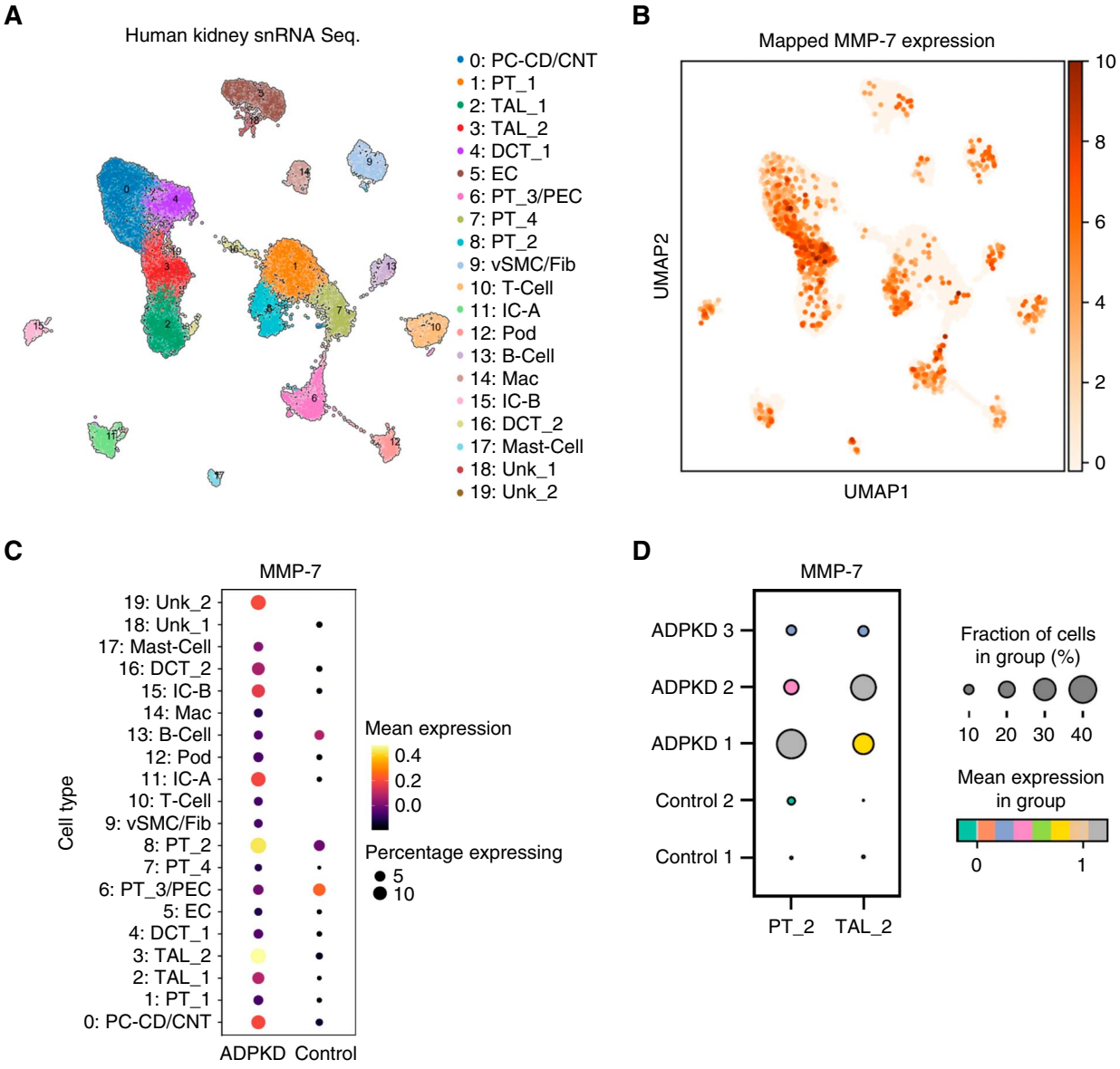

Figure 7. MMP-7 in human ADPKD kidney tissue. Single-nucleus RNA sequencing of human kidneys for 20 different recognized cell types (A) identified MMP-7 for human control and ADPKD tissue when expression was projected on the cell type mapping (B) and directly compared (C) between ADPKD patient kidneys and control tissue. (D) Both the percentage of PT-2 and TAL-2 cells expressing MMP-7 and their mean expression was greater in ADPKD compared with controls. PT, proximal tubule; TAL, thick ascending limb.

tubular level in different forms of AKI and CKD, including ADPKD, progressive IgA nephropathy, and acute kidney transplant rejection, but not in healthy kidney tissue.[40–43] A recent kidney tissue proteomics study identified MMP-7 as a kidney disease biomarker that correlated with fibrosis and predicted faster eGFR decline.[44] The role of MMP-7 in kidney disease appears to be multifactorial. MMP-7 knockout mice show reduced collagen deposition, reduced interstitial fibrosis, but increased albuminuria.[41,45–49] During kidney injury, MMP-7 is upregulated by β-catenin, the principal mediator of canonical Wnt signaling, leading to apoptosis of interstitial fibroblasts, thereby reducing the development of kidney fibrosis.[49] Indeed, MMP-7 knockout mice were more susceptible to ischemia/reperfusion injury and cisplatin, which was reversible when MMP-7 was supplemented.[45] We identified an increase in uEV MMP-7 in rapidly progressive ADPKD in the context of a wider enrichment in Wnt signaling in the pathway analysis of our proteomics data. Polycystins 1 and 2 can both influence Wnt signaling through a number of different intermediates, which in turn could regulate MMP-7. Moreover, in human cyst-lining cells wild-type but not mutated *Pkd1* inhibited β-catenin–mediated Wnt signaling.[50] The interaction between polycystin 2 and the Wnt pathway has been more extensively explored than for

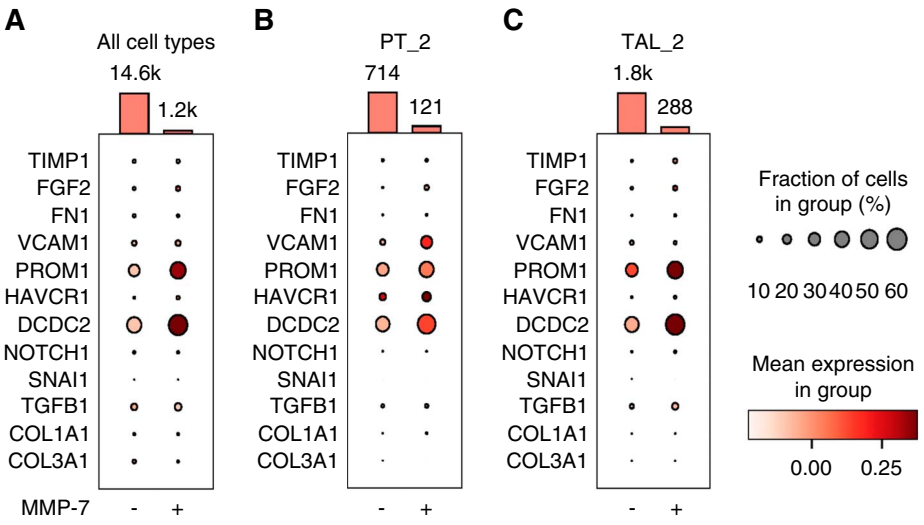

Figure 8. Profibrotic profile of MMP-7 expressing cells. Single-nucleus RNA sequencing of human kidneys recognizes a significantly increased profibrotic expression profile in (A) MMP-7–positive cells for all cell types and those cell types with an increased MMP-7 expression, including (B) PT epithelial cells and (C) TAL cells. COL1A1, collagen type I alpha 1 chain; COL3A1, collagen type III alpha 1 chain; DCDC2, doublecortin domain containing 2; FGF2, fibroblast growth factor 2; FN1, fibronectin 1; HAVCR1, hepatitis A virus cellular receptor 1; NOTCH1; notch receptor 1; PROM1, prominin-1; SNAI1, snail family transcriptional repressor 1; TIMP1, tissue inhibitor of metalloproteinases 1; TGFB1, TGF beta 1; VCAM1, vascular cell adhesion molecule 1.

polycystin 1.[51–54] Loss of *Pkd2* activates β-catenin and stimulates kidney epithelial cell proliferation and cystogenesis. Moreover, inhibition of Wnt and β-catenin suppressed cyst formation in *Pkd2* transgenic mice.[53] In mice, activation of the planar cell polarity pathway, a noncanonical Wnt signaling pathway, precedes cyst development and also includes MMP-7 as a downstream mediator.[54,55] Whether MMP-7 has kidney-protective or detrimental effects in patients with ADPKD warrants further evaluation.

To further analyze the potential role of MMP-7 in ADPKD, we applied snRNA sequencing and found a significantly higher MMP-7 expression in ADPKD tissue than in healthy kidney tissue. Cells with strong MMP-7 expression in ADPKD were located in the proximal tubule and TAL and had a profibrotic phenotype characterized by a strong expression of DCDC2 and PROM1. DCDC2 has previously been implicated in ciliopathies and nephronophthisis and is associated with kidney and liver fibrosis in a Wnt signaling and β-catenin dependent manner.[56–58] PROM1 is increased in the kidney injury response to various stressors and forms protein complexes with E-cadherin and β-catenin.[59] In aging kidneys, a subset of PROM1-positive tubular epithelial cells has been identified that are both functionally impaired and have a distinct profibrotic phenotype.[60]

Our biomarker discovery approach relied on the isolation of uEVs using ultracentrifugation. Ultracentrifugation-based uEV isolation for protein quantification is still the gold standard in the field, but is time-consuming. For this reason, we also tried a commercially available ELISA to quantify MMP-7 in whole urine. Whole-urine MMP-7 measured by ELISA did not show a significant difference between patients with rapid disease progression and stable disease. This implies that uEV-MMP-7 better reflects kidney abundance than whole urine MMP-7, which fits with the concept that EVs are primarily secreted by tubular epithelial cells.[61] Because our study was exploratory, we propose that future studies should validate our findings in a larger ADPKD cohort using a high-throughput platform that does not require the isolation of EVs (*e.g.*, by using fluorescence labeling).[23,62] An analysis of the proteolytic activity of uEV-MMP-7 using zymography would further add to our understanding of its role in ADPKD. Because we identified multiple metalloproteinases in uEVs, this would require MMP-7 purification or the use of a modified zymography assay with MMP-7 specificity.[63]

The strength of this study was the analysis of MMP-7 in six case–control groups that were matched for currently used prognostic markers. A number of limitations, however, should also be mentioned. First, this was an explorative study which was limited by a relatively low number of included patients, which is inherent to the labor-intensive isolation of uEVs using ultracentrifugation. Second, a number of ADPKD-related proteins, including PKD1, PKD2, and hyaluronidase-2 (TMEM2), were either not identified or not different. This is contrast with a previous uEV proteomics study and may be related to differences in sample preparation for mass spectrometry.[11] Third, it is not yet possible to differentiate between normal tubular epithelial cells and cyst-lining epithelial cells when using snRNA sequencing. Finally, the majority of the patients included in this

study had a genetic variant in *PKD1*, and therefore, it is unclear to what degree our findings extend to patients with a *PKD2* variant.

In conclusion, uEV-MMP-7 but not whole-urine MMP-7 is significantly higher in patients with ADPKD who have rapid disease progression compared with those with stable disease. Larger-scale studies using high-throughput, isolation-free methods for uEV-associated MMP-7 are necessary to validate MMP-7 for clinical application as a noninvasive disease progression biomarker in ADPKD.

DISCLOSURES

R.T. Gansevoort reports Consultancy: AstraZeneca, Bayer, Galapagos, Mironid, and Sanofi-Genzyme; Research Funding: AstraZeneca, Abbvie, Bayer, Galapagos, Otsuka Pharmaceuticals, Roche, and Sanofi-Genzyme; Honoraria: Galapagos, Mironid, and Otsuka Pharmaceuticals; and Advisory or Leadership Role: Editor of *American Journal of Kidney Diseases*, *CJASN*, *Journal of Nephrology*, *Kidney360* Member of the Council of the European Renal Association, *Nephron Clinical Practice*, and *Nephrology Dialysis Transplantation*. S. Hayat reports Consultancy: Sequantrix GmbH; Ownership Interest: Sequantrix GmbH; and Research Funding: Askbio GmbH and Novo Nordisk. E.J. Hoorn reports Research Funding: Aurinia; Honoraria: UpToDate; and Advisory or Leadership Role: Editorial Boards: *American Journal of Physiology-Renal Physiology*, *JASN*, and *Journal of Nephrology*; Other committees: Board Member, Dutch Federation of Nephrology and ERA Working Group Genes and Kidney. R. Kramann reports Consultancy: Bayer Healthcare, Gruenenthal, Novo Nordisk, and Pfizer; Research Funding: Chugai, Galapagos, Novo Nordisk, and Travere Therapeutics; Honoraria: Sequantrix; Patents or Royalties: Gli1 cells in fibrosis (method of use); and Advisory or Leadership Role: Board Member and Co-Founder Sequantrix and Scientific Advisory Board Hybridize Therapeutics. E. Meijer reports Research Funding: Dutch Kidney Foundation, Ipsen, Otsuka Pharmaceuticals, Sanofi; all money was paid directly to the institution; and Other Interests or Relationships: Dutch Kidney Foundation, Health Holland, Nieren.nl, NvN, and werkgroep erfelijke nierziekten. R.-U. Müller reports Consultancy: Alnylam and Vifor; Ownership Interest: Bayer and Santa Barbara Nutrients; Research Funding: Otsuka Pharmaceuticals and Thermo Fisher Scientific. All research funding was paid to the employer (Department II of Internal Medicine); Honoraria: Alnylam; Patents or Royalties: Detechgene; and Advisory or Leadership Role: Editorial Board "*Kidney and Dialysis*," Chair of the Board of the Working Group "Genes and Kidney" (ERA), and Scientific Advisory Board Santa Barbara Nutrients. M. Salih reports Advisory or Leadership Role: NedMed.nl Scientific advisory board. M.H. van Heugten reports Research Funding: Aurinia Pharmaceuticals has in part supported our research on lupus nephritis between 2022 and 2023. H. van Willigenburg reports Employer: Antea; and Ownership Interest: funds. All remaining authors have nothing to disclose.

FUNDING

M.H. van Heugten and E.J. Hoorn are supported by Dutch Kidney Foundation grant CP18.05. E.J. Hoorn is also supported by an ERC Consolidator Grant (101125504). The DIPAK consortium is supported by grants from the Dutch Kidney Foundation (grants CP10.12 and CP15.01) and the Dutch Government (LSHM15018). R.-U. Müller is supported by the German Research Foundation (CRU 329, DFG MU 3629/6-1, DFG DI 1501/9, DFG MU 3629/3-1) and the German Federal Ministry of Education and Research (BMBF RNA-STAB) and received research funding from the PKD Foundation (KETO-ADPKD).

AUTHOR CONTRIBUTIONS

Conceptualization: Charles J. Blijdorp, Ewout J. Hoorn, Mahdi Salih, Robert Zietse.
Data curation: Sita Arjune, Karel Bezstarosti, Charles J. Blijdorp, Jeroen A.A. Demmers, Ron T. Gansevoort, Sikander Hayat, Esther Meijer, Roman-Ulrich Müller, Usha Musterd-Bhaggoe, Martijn H. van Heugten.
Formal analysis: Charles J. Blijdorp, Sikander Hayat, Ewout J. Hoorn, Martijn H. van Heugten.
Funding acquisition: Ewout J. Hoorn.
Investigation: Karel Bezstarosti, Charles J. Blijdorp, Jeroen A.A. Demmers, Usha Musterd-Bhaggoe, Martijn H. van Heugten.
Methodology: Karel Bezstarosti, Charles J. Blijdorp, Jeroen A.A. Demmers, Sikander Hayat, Ewout J. Hoorn, Rafael Kramann, Usha Musterd-Bhaggoe, Martijn H. van Heugten.
Project administration: Ewout J. Hoorn.
Resources: Ewout J. Hoorn.
Software: Martijn H. van Heugten.
Supervision: Ewout J. Hoorn, Rafael Kramann, Roman-Ulrich Müller, Mahdi Salih, Hester van Willigenburg, Robert Zietse.
Validation: Sita Arjune, Ron T. Gansevoort, Ewout J. Hoorn, Esther Meijer, Roman-Ulrich Müller, Mahdi Salih.
Visualization: Sikander Hayat, Martijn H. van Heugten.
Writing – original draft: Ewout J. Hoorn, Martijn H. van Heugten.
Writing – review & editing: Sita Arjune, Karel Bezstarosti, Charles J. Blijdorp, Jeroen A.A. Demmers, Ron T. Gansevoort, Sikander Hayat, Rafael Kramann, Esther Meijer, Roman-Ulrich Müller, Usha Musterd-Bhaggoe, Mahdi Salih, Hester van Willigenburg, Robert Zietse.

DATA SHARING STATEMENT

Data related to transcriptomic, proteomic, or metabolomic data (per previous question). All data is included in the manuscript and/or supporting information.

SUPPLEMENTAL MATERIAL

This article contains the following supplemental material online at http://links.lww.com/JSN/E560.

Supplemental Table 1. Characteristics of discovery groups 1 and 2.
Supplemental Table 2. Characteristics of internal validation group 3.
Supplemental Table 3. Characteristics of internal validation group 4.
Supplemental Table 4. Characteristics of external validation groups 5 and 6.
Supplemental Table 5. Significant proteins from discovery group 1 sorted by fold change.
Supplemental Table 6. Significant proteins from discovery group 2 sorted by fold change.
Supplemental Table 7. Regression analysis to analyze the association between whole-urine MMP-7 and eGFR loss.
Supplemental Figure 1. Heat map of significant proteins from discovery groups 1 and 2.
Supplemental Figure 2. Immunoblot results in group 3 when normalized to CD9.
Supplemental Figure 3. Receiver operating characteristic curves for validation groups 3 and 6.
Supplemental Figure 4. Correlation of uEV and whole-urine MMP-7 in internal validation group 3.
Supplemental Figure 5. uEV-MMP-7 abundance measured by MS/MS in healthy individuals and in patients with CKD and ADPKD.
Supplemental Data 1. Cohort 1 significant differentially abundant proteins by MS/MS ranked by (absolute) fold change (FC).

REFERENCES

1. Bergmann C, Guay-Woodford LM, Harris PC, Horie S, Peters DJM, Torres VE. Polycystic kidney disease. *Nat Rev Dis Primers*. 2018;4(1):50. doi:10.1038/s41572-018-0047-y
2. Cornec-Le Gall E, Torres VE, Harris PC. Genetic complexity of autosomal dominant polycystic kidney and liver diseases. *J Am Soc Nephrol*. 2018;29(1):13–23. doi:10.1681/ASN.2017050483
3. Lanktree MB, Guiard E, Li W, et al. Intrafamilial variability of ADPKD. *Kidney Int Rep*. 2019;4(7):995–1003. doi:10.1016/j.ekir.2019.04.018
4. Cornec-Le Gall E, Alam A, Perrone RD. Autosomal dominant polycystic kidney disease. *Lancet*. 2019;393(10174):919–935. doi:10.1016/S0140-6736(18)32782-X
5. Gansevoort RT, Arici M, Benzing T, et al. Recommendations for the use of tolvaptan in autosomal dominant polycystic kidney disease: a position statement on behalf of the ERA-EDTA Working Groups on Inherited Kidney Disorders and European Renal Best Practice. *Nephrol Dial Transplant*. 2016;31(3):337–348. doi:10.1093/ndt/gfv456
6. Irazabal MV, Rangel LJ, Bergstralh EJ, et al.; CRISP Investigators. Imaging classification of autosomal dominant polycystic kidney disease: a simple model for selecting patients for clinical trials. *J Am Soc Nephrol*. 2015;26(1):160–172. doi:10.1681/ASN.2013101138
7. Erdbrügger U, Blijdorp CJ, Bijnsdorp IV, et al. Urinary extracellular vesicles: a position paper by the urine task force of the International Society for extracellular vesicles. *J Extracell Vesicles*. 2021;10(7):e12093. doi:10.1002/jev2.12093
8. Wu Q, Poulsen SB, Murali SK, et al. Large-scale proteomic assessment of urinary extracellular vesicles highlights their reliability in reflecting protein changes in the kidney. *J Am Soc Nephrol*. 2021;32(9):2195–2209. doi:10.1681/ASN.2020071035
9. Salih M, Demmers JA, Bezstarosti K, et al.; DIPAK Consortium. Proteomics of urinary vesicles links plakins and complement to polycystic kidney disease. *J Am Soc Nephrol*. 2016;27(10):3079–3092. doi:10.1681/ASN.2015090994
10. Bruschi M, Granata S, Santucci L, et al. Proteomic analysis of urinary microvesicles and exosomes in medullary sponge kidney disease and autosomal dominant polycystic kidney disease. *Clin J Am Soc Nephrol*. 2019;14(6):834–843. doi:10.2215/CJN.12191018
11. Hogan MC, Bakeberg JL, Gainullin VG, et al. Identification of biomarkers for PKD1 using urinary exosomes. *J Am Soc Nephrol*. 2015;26(7):1661–1670. doi:10.1681/ASN.2014040354
12. Kistler AD, Serra AL, Siwy J, et al. Urinary proteomic biomarkers for diagnosis and risk stratification of autosomal dominant polycystic kidney disease: a multicentric study. *PLoS One*. 2013;8(1):e53016. doi:10.1371/journal.pone.0053016
13. Song CJ, Zimmerman KA, Henke SJ, Yoder BK. Inflammation and fibrosis in polycystic kidney disease. *Results Probl Cell Differ*. 2017;60:323–344. doi:10.1007/978-3-319-51436-9_12
14. Wang J, Nikonorova IA, Gu A, Sternberg PW, Barr MM. Release and targeting of polycystin-2-carrying ciliary extracellular vesicles. *Curr Biol*. 2020;30(13):R755–R756. doi:10.1016/j.cub.2020.05.079
15. Raby KL, Horsely H, McCarthy-Boxer A, Norman JT, Wilson PD. Urinary exosome proteomic profiling defines stage-specific rapid progression of autosomal dominant polycystic kidney disease and tolvaptan efficacy. *BBA Adv*. 2021;1:100013. doi:10.1016/j.bbadva.2021.100013
16. Meijer E, Drenth JP, d'Agnolo H, et al.; DIPAK Consortium. Rationale and design of the DIPAK 1 study: a randomized controlled clinical trial assessing the efficacy of lanreotide to Halt disease progression in autosomal dominant polycystic kidney disease. *Am J Kidney Dis*. 2014;63(3):446–455. doi:10.1053/j.ajkd.2013.10.011
17. Meijer E, Visser FW, van Aerts RMM, et al.; DIPAK-1 Investigators. Effect of lanreotide on kidney function in patients with autosomal dominant polycystic kidney disease: the DIPAK 1 randomized clinical trial. *JAMA*. 2018;320(19):2010–2019. doi:10.1001/jama.2018.15870
18. Pisitkun T, Shen RF, Knepper MA. Identification and proteomic profiling of exosomes in human urine. *Proc Natl Acad Sci U S A*. 2004;101(36):13368–13373. doi:10.1073/pnas.0403453101
19. van der Lubbe N, Jansen PM, Salih M, et al. The phosphorylated sodium chloride cotransporter in urinary exosomes is superior to prostasin as a marker for aldosteronism. *Hypertension*. 2012;60(3):741–748. doi:10.1161/HYPERTENSIONAHA.112.198135
20. Braun F, Rinschen M, Buchner D, et al. The proteomic landscape of small urinary extracellular vesicles during kidney transplantation. *J Extracell Vesicles*. 2020;10(1):e12026. doi:10.1002/jev2.12026
21. Hughes CS, Moggridge S, Müller T, Sorensen PH, Morin GB, Krijgsveld J. Single-pot, solid-phase-enhanced sample preparation for proteomics experiments. *Nat Protoc*. 2019;14(1):68–85. doi:10.1038/s41596-018-0082-x
22. Kalra H, Simpson RJ, Ji H, et al. Vesiclepedia: a compendium for extracellular vesicles with continuous community annotation. *PLoS Biol*. 2012;10(12):e1001450. doi:10.1371/journal.pbio.1001450
23. Blijdorp CJ, Tutakhel OAZ, Hartjes TA, et al. Comparing approaches to normalize, quantify, and characterize urinary extracellular vesicles. *J Am Soc Nephrol*. 2021;32(5):1210–1226. doi:10.1681/ASN.2020081142
24. Xu Y, Kuppe C, Perales-Patón J, et al. Adult human kidney organoids originate from CD24(+) cells and represent an advanced model for adult polycystic kidney disease. *Nat Genet*. 2022;54(11):1690–1701. doi:10.1038/s41588-022-01202-z
25. Kramann R, Machado F, Wu H, et al. Parabiosis and single-cell RNA sequencing reveal a limited contribution of monocytes to myofibroblasts in kidney fibrosis. *JCI Insight*. 2018;3(9):e99561. doi:10.1172/jci.insight.99561
26. Kuppe C, Ramirez Flores RO, Li Z, et al. Spatial multi-omic map of human myocardial infarction. *Nature*. 2022;608(7924):766–777. doi:10.1038/s41586-022-05060-x
27. El-Achkar TM, Eadon MT, Menon R, et al. A multimodal and integrated approach to interrogate human kidney biopsies with rigor and reproducibility: guidelines from the Kidney Precision Medicine Project. *Physiol Genomics*. 2021;53(1):1–11. doi:10.1152/physiolgenomics.00104.2020
28. Huang R, Fu P, Ma L. Kidney fibrosis: from mechanisms to therapeutic medicines. *Signal Transduct Target Ther*. 2023;8(1):129. doi:10.1038/s41392-023-01379-7
29. Huber W, von Heydebreck A, Sültmann H, Poustka A, Vingron M. Variance stabilization applied to microarray data calibration and to the quantification of differential expression. *Bioinformatics*. 2002;18(suppl 1):S96–S104. doi:10.1093/bioinformatics/18.suppl_1.s96
30. Välikangas T, Suomi T, Elo LL. A systematic evaluation of normalization methods in quantitative label-free proteomics. *Brief Bioinform*. 2018;19(1):1–11. doi:10.1093/bib/bbw095
31. Fabregat A, Sidiropoulos K, Viteri G, et al. Reactome pathway analysis: a high-performance in-memory approach. *BMC Bioinformatics*. 2017;18(1):142. doi:10.1186/s12859-017-1559-2
32. Jassal B, Matthews L, Viteri G, et al. The reactome pathway knowledgebase. *Nucleic Acids Res*. 2020;48(D1):D498–D503. doi:10.1093/nar/gkz1031
33. Venkatraman ES. A permutation test to compare receiver operating characteristic curves. *Biometrics*. 2000;56(4):1134–1138. doi:10.1111/j.0006-341x.2000.01134.x
34. Jamadar A, Suma SM, Mathew S, et al. The tyrosine-kinase inhibitor Nintedanib ameliorates autosomal-dominant polycystic kidney disease. *Cell Death Dis*. 2021;12(10):947. doi:10.1038/s41419-021-04248-9
35. Kim S, Nie H, Nesin V, et al. The polycystin complex mediates Wnt/Ca(2+) signalling. *Nat Cell Biol*. 2016;18(7):752–764. doi:10.1038/ncb3363
36. Parker E, Newby LJ, Sharpe CC, et al. Hyperproliferation of PKD1 cystic cells is induced by insulin-like growth factor-1 activation of the Ras/Raf

signalling system. *Kidney Int.* 2007;72(2):157–165. doi:10.1038/sj.ki.5002229
37. Sankaran D, Bankovic-Calic N, Ogborn MR, Crow G, Aukema HM. Selective COX-2 inhibition markedly slows disease progression and attenuates altered prostanoid production in Han:SPRD-cy rats with inherited kidney disease. *Am J Physiol Renal Physiol.* 2007;293(3):F821–F830. doi:10.1152/ajprenal.00257.2006
38. Liu Z, Tan RJ, Liu Y. The many faces of matrix metalloproteinase-7 in kidney diseases. *Biomolecules.* 2020;10(6):960. doi:10.3390/biom10060960
39. Wozniak J, Floege J, Ostendorf T, Ludwig A. Key metalloproteinase-mediated pathways in the kidney. *Nat Rev Nephrol.* 2021;17(8):513–527. doi:10.1038/s41581-021-00415-5
40. Zhang J, Ren P, Wang Y, et al. Serum matrix metalloproteinase-7 level is associated with fibrosis and renal survival in patients with IgA nephropathy. *Kidney Blood Press Res.* 2017;42(3):541–552. doi:10.1159/000477132
41. Zhou D, Tian Y, Sun L, et al. Matrix metalloproteinase-7 is a urinary biomarker and pathogenic mediator of kidney fibrosis. *J Am Soc Nephrol.* 2017;28(2):598–611. doi:10.1681/ASN.2016030354
42. Jovanovic V, Dugast AS, Heslan JM, et al. Implication of matrix metalloproteinase 7 and the noncanonical wingless-type signaling pathway in a model of kidney allograft tolerance induced by the administration of anti-donor class II antibodies. *J Immunol.* 2008;180(3):1317–1325. doi:10.4049/jimmunol.180.3.1317
43. Surendran K, Simon TC, Liapis H, McGuire JK. Matrilysin (MMP-7) expression in renal tubular damage: association with Wnt4. *Kidney Int.* 2004;65(6):2212–2222. doi:10.1111/j.1523-1755.2004.00641.x
44. Hirohama D, Abedini A, Moon S, et al. Unbiased human kidney tissue proteomics identifies matrix metalloproteinase 7 as a kidney disease biomarker. *J Am Soc Nephrol.* 2023;34(7):1279–1291. doi:10.1681/ASN.0000000000000141
45. Fu H, Zhou D, Zhu H, et al. Matrix metalloproteinase-7 protects against acute kidney injury by priming renal tubules for survival and regeneration. *Kidney Int.* 2019;95(5):1167–1180. doi:10.1016/j.kint.2018.11.043
46. Obermüller N, Morente N, Kränzlin B, Gretz N, Witzgall R. A possible role for metalloproteinases in renal cyst development. *Am J Physiol Renal Physiol.* 2001;280(3):F540–F550. doi:10.1152/ajprenal.2001.280.3.F540
47. Riera M, Burtey S, Fontés M. Transcriptome analysis of a rat PKD model: importance of genes involved in extracellular matrix metabolism. *Kidney Int.* 2006;69(9):1558–1563. doi:10.1038/sj.ki.5000309
48. Tan RJ, Li Y, Rush BM, et al. Tubular injury triggers podocyte dysfunction by beta-catenin-driven release of MMP-7. *JCI Insight.* 2019;4(24):e122399. doi:10.1172/jci.insight.122399
49. Zhou D, Tan RJ, Zhou L, Li Y, Liu Y. Kidney tubular beta-catenin signaling controls interstitial fibroblast fate via epithelial-mesenchymal communication. *Sci Rep.* 2013;3:1878. doi:10.1038/srep01878
50. Lal M, Song X, Pluznick JL, et al. Polycystin-1 C-terminal tail associates with beta-catenin and inhibits canonical Wnt signaling. *Hum Mol Genet.* 2008;17(20):3105–3117. doi:10.1093/hmg/ddn208
51. Kim E, Arnould T, Sellin LK, et al. The polycystic kidney disease 1 gene product modulates Wnt signaling. *J Biol Chem.* 1999;274(8):4947–4953. doi:10.1074/jbc.274.8.4947
52. Le NH, van der Bent P, Huls G, et al. Aberrant polycystin-1 expression results in modification of activator protein-1 activity, whereas Wnt signaling remains unaffected. *J Biol Chem.* 2004;279(26):27472–27481. doi:10.1074/jbc.M312183200
53. Li A, Xu Y, Fan S, et al. Canonical Wnt inhibitors ameliorate cystogenesis in a mouse ortholog of human ADPKD. *JCI Insight.* 2018;3(5):e95874. doi:10.1172/jci.insight.95874
54. Qin S, Taglienti M, Cai L, Zhou J, Kreidberg JA. c-Met and NF-κB-dependent overexpression of Wnt7a and -7b and Pax2 promotes cystogenesis in polycystic kidney disease. *J Am Soc Nephrol.* 2012;23(8):1309–1318. doi:10.1681/ASN.2011030277
55. Luyten A, Su X, Gondela S, et al. Aberrant regulation of planar cell polarity in polycystic kidney disease. *J Am Soc Nephrol.* 2010;21(9):1521–1532. doi:10.1681/ASN.2010010127
56. Ge WS, Wang YJ, Wu JX, Fan JG, Chen YW, Zhu L. β-catenin is overexpressed in hepatic fibrosis and blockage of Wnt/β-catenin signaling inhibits hepatic stellate cell activation. *Mol Med Rep.* 2014;9(6):2145–2151. doi:10.3892/mmr.2014.2099
57. Otto EA, Schermer B, Obara T, et al. Mutations in INVS encoding inversin cause nephronophthisis type 2, linking renal cystic disease to the function of primary cilia and left-right axis determination. *Nat Genet.* 2003;34(4):413–420. doi:10.1038/ng1217
58. Schueler M, Braun DA, Chandrasekar G, et al. DCDC2 mutations cause a renal-hepatic ciliopathy by disrupting Wnt signaling. *Am J Hum Genet.* 2015;96(1):81–92. doi:10.1016/j.ajhg.2014.12.002
59. Brossa A, Papadimitriou E, Collino F, et al. Role of CD133 molecule in Wnt response and renal repair. *Stem Cells Transl Med.* 2018;7(3):283–294. doi:10.1002/sctm.17-0158
60. Eymael J, van den Broek M, Miesen L, et al. Human scattered tubular cells represent a heterogeneous population of glycolytic dedifferentiated proximal tubule cells. *J Pathol.* 2023;259(2):149–162. doi:10.1002/path.6029
61. Blijdorp CJ, Hartjes TA, Wei KY, et al. Nephron mass determines the excretion rate of urinary extracellular vesicles. *J Extracell Vesicles.* 2022;11(1):e12181. doi:10.1002/jev2.12181
62. Tian Y, Gong M, Hu Y, et al. Quality and efficiency assessment of six extracellular vesicle isolation methods by nano-flow cytometry. *J Extracell Vesicles.* 2020;9(1):1697028. doi:10.1080/20013078.2019.1697028
63. Tajhya RB, Patel RS, Beeton C. Detection of matrix metalloproteinases by zymography. *Methods Mol Biol.* 2017;1579:231–244. doi:10.1007/978-1-4939-6863-3_12

AFFILIATIONS

[1]Division of Nephrology and Transplantation, Department of Internal Medicine, Erasmus Medical Center, Rotterdam, The Netherlands
[2]Department II of Internal Medicine and Center for Molecular Medicine, University of Cologne, Cologne, Germany
[3]Cologne Excellence Cluster on Cellular Stress Responses in Aging-Associated Diseases (CECAD), Faculty of Medicine and University Hospital Cologne, University of Cologne, Cologne, Germany
[4]Faculty of Medicine and University Hospital Cologne, Center for Rare Diseases Cologne, University of Cologne, Cologne, Germany
[5]Proteomics Center, Erasmus Medical Center, Rotterdam, The Netherlands
[6]Department of Internal Medicine, University Medical Center Groningen, Groningen, The Netherlands
[7]Medical Faculty, Institute of Experimental Medicine and Systems Biology, RWTH Aachen University, Aachen, Germany
[8]Division of Nephrology, RWTH Aachen University, Aachen, Germany